EUROPEAN FUSION DEVELOPMENT AGREEMENT

JET

EFDA–JET–PR(04)74

I. Voitsekhovitch, K.-D. Zastrow, B. Alper, G. Bonheure, X. Garbet,
V. Kiptily, E. de la Luna, D. McCune, D. McDonald, S. Popovichev,
S.E. Sharapov, D. Stork, and JET-EFDA Contributors

Effect of Sawtooth Activity on Tritium and Beam Deuterium Evolution in Trace Tritium Experiments on JET

Effect of Sawtooth Activity on Tritium and Beam Deuterium Evolution in Trace Tritium Experiments on JET

I. Voitsekhovitch[1], K.-D. Zastrow[1], B. Alper[1], G. Bonheure[2], X. Garbet[3], V. Kiptily[1], E. de la Luna[4], D. McCune[5], D. McDonald[1], S. Popovichev[1], S.E. Sharapov[1], D. Stork[1], and JET-EFDA Contributors*

[1]*EURATOM/UKAEA Fusion Association, Culham Science Centre, Abingdon, UK*
[2]*LPP-ERM KMS Association EURATOM/Belgian State, Brussels, Belgium*
[3]*Association EURATOM/CEA Cadarache, F-13108, St Paul lez Durance, France*
[4]*Laboratorio Nacional de Fusion, Asociacion EURATOM-CIEMAT, Madrid, Spain*
[5]*PPPL, Princeton University, Princeton, NJ, 08543, USA*
** See annex of J. Pamela et al, "Overview of Recent JET Results and Future Perspectives", Fusion Energy 2002 (Proc.19 th IAEA Fusion Energy Conference, Lyon (2002)).*

Preprint of Paper to be submitted for publication in
Plasma Physics and Controlled Fusion

ABSTRACT

One of the scenarios actively studied during the recent trace tritium experimental campaign performed on JET includes a gas puff of small amounts of tritium into the sawtooth-unstable H-mode plasmas heated by deuterium beams. The sawtooth crashes observed in these discharges with the Electron Cyclotron Emission (ECE) diagnostics are frequently accompanied by the oscillations of the 14MeV neutron emission produced mainly due to the reaction between deuterium beam and thermal tritium. Such oscillations are clearly seen in low density plasma while they are weak or absent at high density. The dynamics of the trace tritium and beam deuterium during the sawtooth crash is studied here numerically using the TRANSP code with the goal to explain the different evolution of neutron emission with density. A test of the full and partial reconnection models in predictive simulations of neutron data with the TRANSP code is discussed.

1. INTRODUCTION

The sawtooth oscillation, i.e., the periodic oscillation of core electron temperature and density occurring when the central safety factor q_0 drops below unity - is one of the most frequent MHD activity in tokamak plasma [1 - 12]. The expulsion of particles and energy from the plasma core during the sawtooth crash can affect the overall plasma confinement and trigger edge localised modes (ELMs). Such expulsion is caused by the development and growth of a magnetic island with subsequent full [13] or partial [14 - 16] reconnection of magnetic field lines.

The sawtooth instability affects different minority plasma species in addition to main species [7, 8, 17, 18]. It prevents an impurity accumulation and maintains a flat Argon (Ar) profile in JET discharges with Ar seeding [7, 8]. The fast hydrogen ions in TFTR discharges with Ion Cyclotron Resonance Heating (ICRH) are redistributed from the plasma core to well beyond the q = 1 surface by sawtooth crashes where their increased losses are observed due to magnetic field ripples [17, 18]. The sawtooth oscillations, considered routinely as a mechanism of particle losses, play a different role in experiments with short edge fuelling, such as the injection of impurities by laser blow-off [2, 4] or single gas puff of trace species [19, 20]. The metallic impurities (Ni, Mo) injected from the plasma edge in JET L-mode plasmas exhibit an off-axis deposition profile until the sawtooth collapse brings them into the plasma core [2, 4]. The experiments performed recently on JET by puffing small amounts of tritium into deuterium H-mode plasmas [19, 20] show that, the sawtooth crashes accelerate the penetration of tritium into the plasma core at the beginning of the puff when the tritium profile is still hollow [21]. As soon as the tritium fills the plasma volume and forms a peaked profile, the sawtooth activity enhances the core tritium losses as well as the losses of other plasma species. Similar behaviour of Argon has been reported in Ref. 7.

In trace tritium experiments analysed here the sawtooth activity, detected as the oscillations of electron temperature measured by the multi-channel Electron Cyclotron Emission (ECE) diagnostics, is observed in H-mode plasmas at different density. In low density plasmas ($n_e \approx (2 - 4)10^{19}\ m^{-3}$), the sawtooth crashes are accompanied by the oscillations of the 14MeV neutron emission from the neutrons produced by the deuterium-tritium (DT) reaction. These oscillations become weaker at medium density ($n_e \approx (5 - 6)10^{19}$ m^{-3}) and disappear at high density ($n_e \approx (9 - 10)10^{19}$ m-3). This effect, i.e., the different behaviour of neutron emission with density during the sawtooth collapse in plasmas with equally strong sawtooth activity as measured by the ECE diagnostic is the subject of the present study. The analysis of this phenomenon is performed via predictive simulations of plasma neutron emission along the lines of sight of the JET neutron camera with the TRANSP code [22, 23].

The TRANSP simulations show that the main contribution to the 14MeV neutron emission is produced by the neutrons born in the reaction between the trace tritium and beam deuterium. Therefore, the different evolution of the neutron emission at low and high plasma density indicates to a different behaviour of these species. Since the trace tritium transport and beam-plasma interaction are simulated in TRANSP, the proper prediction of the oscillations of neutron emission gives an additional test for the models describing these processes. The strong sawtooth mixing of these species at low density resulting in strong oscillations of neutron emission is sensitive to the positions of the inversion radius that can be used also for a rough estimation of the qprofile modification during the sawtooth collapse. The possibility to compare the full [13] and partial reconnection as it is implemented in TRANSP by performing a sensitivity study for low density plasma will be discussed.

This paper is organised as follows. After the brief description of experimental scenarios, diagnostics and analysis method (Section II) the effect of sawtooth oscillations on the evolution of deuterium beam and trace tritium is analysed in detail at low density (Section III). In Section IV, the simulations of neutron emission in high density plasma are described. The results of this study are briefly summarised in Section V.

2. EXPERIMENTAL CONDITIONS, DIAGNOSTICS AND ANALYSIS METHOD

The experiments with the tritium gas puff into steady-state H-mode plasmas have been performed in the following range of magnetic fields B_t = 1.65 – 2.25T, plasma currents I_{pl} = 2 – 2.5MA, deuterium neutral beam powers P_{nbi} = 2.3 – 14 MW and central line averaged densities $n_l = (2.4 - 9)10^{19}$ m^{-3}, where the sawtooth activity is frequently observed. Sawteeth are detected as oscillations of electron temperature measured by the ECE diagnostics with 0.4ms time resolution. The amplitude of the core temperature oscillations ΔT_e is 10 – 20% and the period between the oscillations varies within 240 - 400ms. The reconnection occurs rapidly producing a sharp temperature reduction in 0.5 - 0.8ms.

For more detailed analysis of sawtooth effect, two discharges performed at low and high plasma density, but at nearly the same sawtooth amplitude ΔT_e have been selected. Parameters of these pulses are given in Table I, and the comparison between the characteristic plasma time scales estimated at the q = 1 surface (such as energy confinement time, resistive and electron collision time) and the times of sawtooth relaxation and collapse is presented in Table II. The energy confinement time is estimated in TRANSP using the computed heat deposition profiles (NBI and ohmic (for electrons) heating), electron-ion energy exchange, energy losses due to atomic processes and measured temperature and density profiles. The resistive time $\tau_R = 4\pi r_{q=1}{}^{-2} / \eta_{//} c^2$ is calculated with parallel Spitzer resistivity, η_{Sp}, completed with the neoclassical correction, which takes into account trapped particles, $\eta / = \eta_{Sp} / (1 - 2(r_{q=1}/R)^{0.5})$. As follows from Table II, the time of the sawtooth collapse is much shorter than the Kadomtsev reconnection time, $(\tau_A \tau_R)^{1/2} \sim 3$ - 4ms. Similar results have been obtained in other tokamaks [9, 11]. The fast sawtooth collapse may be understood taking into account the electron inertia in the estimation of the reconnection layer [24, 25]. At low density, the sawtooth crash occurs in a time scale comparable to electron collisional time suggesting that the collisional reconnection mechanism cannot fully account for reconnection while the collisions become important at high density. The sawtooth relaxation time is close to the energy confinement time indicating that the sawtooth threshold may be associated with a critical pressure gradient.

The oscillations of the electron temperature in selected pulses are shown in Fig.1 together with the evolution of the 14MeV neutron yield measured by the neutron detector with 10ms time resolution. The profile of neutron emission is obtained with the neutron camera, which performs the measurements along the 10 horizontal and 9 vertical chords with the same time resolution (Fig.2) [26]. The plasma density in these pulses is measured with the Thomson scattering diagnostic along the 50 channels with 250ms time resolution. This diagnostic is used also for the measurement of electron temperature profile in the high density discharge where the ECE measurements are available only in the plasma core. The temperature of carbon impurity and effective charge of the plasma are measured by the Charge eXchange (CX) diagnostic along the 9 chords with 50ms time resolution. The time of each sawtooth crash is determined from the oscillations of electron temperature measured by the ECE diagnostics and introduced in TRANSP.

The analysis of sawtooth crashes is performed by predicting the evolution of the measured neutron emission along the 19 chords and the total neutron yield in TRANSP simulations. The DT neutron emission is produced mainly by the reaction between the beam deuterium and thermal tritium that requires an accurate estimation of the concentration of these species. The neutral beam deposition and the profile of fast deuterium are calculated by using the Monte-Carlo procedure implemented in TRANSP [27]. The tritium evolution is obtained by solving the tritium continuity equation, where the tritium diffusion coefficient and convective velocity are prescribed and the sources are calculated in TRANSP. The algorithm for the estimation of tritium transport coefficients from the least-square fit of transport model to measured neutron emission is described elsewhere [19], and here we use the transport coefficients obtained with this technique. The profiles of the volume and wall recycling sources of tritium are estimated using the FRANTIC code [28] built into TRANSP. The more detailed description of the model and approach used for the analysis of trace tritium transport is given in Ref. 29.

The sawtooth crashes are simulated using the Kadomtsev reconnection model [13] implemented in TRANSP [23]. This model estimates the sawtooth inversion radius r_{inv} at the time of each crash. The q-profile is modified after the crash so that $q = 1$ at $r < r_{inv}$. The evolution of the q-profile between the crashes is simulated in TRANSP using the current diffusion equation with neoclassical conductivity and bootstrap current taken from NCLASS. The profile of beam ions is modified during the crash following the shift of magnetic flux surfaces estimated with the Kadomtsev helical flux mixing algorithm. The measured electron temperature displaying the sawtooth oscillations is used in simulations. The temperature of the main ion species is calculated from the measured CX temperature. The conservation of particles and total ion energy during the crash determines the re-distribution of bulk deuterium and trace tritium.

The sawtooth model described above corresponds to the complete reconnection of flux surfaces [13]. However, the experimental observations [5, 6, 9] and theoretical studies [14 – 16, 24] indicate that the physics of reconnection process is more complicated. If the reconnection is accompanied by the destabilisation of magnetic turbulence (for example, due to toroidal coupling of the n = 1, m = 1 mode with the satellite harmonics of magnetic perturbations localised within the q = 1 surface, such as n = 2, m = 2) the boundary of magnetic island will be destroyed and the full reconnection will be prevented. The heuristic model describing such processes predicts a rapid return of initially shifted core region with $q < 1$ to the centre and the formation of the layer between the core and mixing radius where the reconnection flattens the q-profile. Thus, the q-profile after the crash is supposed to have a shoulder with q = 1 surrounding the core region with $q < 1$. The evolution of energy and particle transport during the incomplete reconnection is rather complicated: the conservation of the core region with $q < 1$ can reduce the plasma expulsion from the centre while the pressure profile may still be flattened due to an enhanced transport in stochastic region. The sawtooth model implemented in TRANSP has the possibility to describe a situation similar to the incomplete reconnection, where the q-profile is maintained below unity in the core. This is done by imposing a weighted average of the unmixed and fully mixed current profile after the crash. However, a shoulder with q = 1 characterising the incomplete reconnection is not reproduced in such model, and the q-profile has a small, but non-zero gradient inside the inversion radius. Such evolution of q-profile is accompanied in the TRANSP sawtooth model either by the same energy and particle mixing like in the full reconnection model, or the beam mixing can be turned on or off. In what follows these options are used to illustrate the effect of current diffusion and beam particle mixing on the oscillations of neutron emission.

3. SAWTOOTH MIXING OF DIFFERENT PLASMA SPECIES AT LOW DENSITY

At low density, the ECE oscillations correlate with the oscillations of the total DT neutron yield (Fig.1(a)) and neutron emission measured along the chords n° 1 – 7 and 11 – 18 (the oscillations observed along the horizontal chords n° 4 - 7 are shown in Fig.3). The oscillations of the neutron emission depend explicitly on the mixing of ion energy, beam and thermal deuterium and trace tritium. The fractions of redistributed energy and particles depend on the current profile before the crash, and therefore on the electron temperature dependent current conductivity. While the electron and ion temperature are taken from the measurements, the different assumptions on the mixing of plasma current and beam particles will be tested here in predictive simulations of neutron emission.

First, the simulations of neutron emission have been performed taking into account the sawtooth mixing of all plasma species and assuming the full reconnection of magnetic field lines with q = 1 inside the inversion radius after the crash. The simulated neutron emission is compared in Fig.3 (top panel) with the measurements for 6 horizontal chords. The full reconnection model used in TRANSP reproduces both the drop of the neutron emission in the centre and its increase on the outer chords outside the inversion radius during the decay phase. The Fig.3 includes also the simulations performed without the sawtooth crashes (bottom panel). The comparison between two cases shown on the top and bottom panels clearly shows the importance of the sawtooth mixing for more accurate prediction of the neutron emission.

The evolution of plasma profiles during the sawtooth crash simulated with the full reconnection model is shown in Figs.4 - 7. The central safety factor reduces from 1 to 0.9 between the sawteeth while it would drop to 0.5 in the simulations performed without the sawtooth crashes (Fig.4, dotted curve). The position of the q = 1 radius before the crash calculated in TRANSP is around 0.5. This location of the q = 1 surface has been verified with the ECE and soft X-ray measurements and the magnetic probe measurements showing the evolution of the n = 1, m = 1 mode. The normalised inversion radius determined from the evolution of electron temperature profile during the crash is around 0.35 that is in agreement with the soft X-ray data. The magnetic probes detected the n = 1, m = 1 mode with the frequency 5.5 – 6.0kHz. Taking into account the toroidal rotation profile from the CX measurements the position of this mode can be estimated as r/a = 0.45 – 0.50 (the error bars of CX rotation data are taken into account in this estimation). Thus, the soft X-ray and ECE data give slightly smaller value of the inversion radius than the magnetic probe and CX measurements. The measurements of the neutron emission displaying the inversion of the oscillations along the chords located between r/a = 0.23 and 0.51 (n°3 and 7) do not allow a more precise estimation of the inversion radius.

The typical re-distribution of beam particles during the sawtooth crash is shown in Fig.5. In low density plasma the neutral beams easily penetrate to the plasma core and the beam particle profile is peaked before the crash (Fig.5, solid curve). The fraction of beam particles removed from the centre during the crash is relatively large in this case. These particles frozen in the corresponding flux surfaces are rapidly shifted toward the edge during the helical flux mixing forming the profile with an off-axis peak (Fig.5, dashed curve). The re-distribution of trace tritium during the sawtooth crash also depends on its profile inside the inversion radius. At the beginning of the puff when the tritium density profile is still hollow the flux reconnection provides a rapid tritium penetration from the boundary of the mixing region to the plasma centre, and the central tritium density exhibits a step-like rise (Fig.6). However, this rise of central tritium density may not be accompanied by the rise of the neutron emission because of the simultaneous removal of beam particles from the plasma core (Fig.5 and Fig.6 (dashed curve)). Later, when the peaked tritium density profile is formed (this time can be roughly estimated as a time of the peak of the neutron emission) the sawtooth crashes lead to the similar evolution of beam particles and trace tritium removing both species from the plasma core. The oscillations of neutron emission become very strong during this phase (Fig. 3).

The evolution of tritium density profile caused by the sawtooth crash occurring during the rise and decay phases of neutron emission is shown in Fig.7.

The comparison of the fractions of beam particles and trace tritium involved in the reconnection process (Figs.5 and 7) shows that the beam mixing possibly provides the main contribution to the oscillations of neutron emission. The effect of the beam mixing can be illustrated by comparing the simulations of the neutron emission performed with and without the beam particle re-distribution during the sawtooth crash while keeping the same mixing of other plasma species and current density. These simulations are shown in Figure 8 for the central horizontal chord and chord n°7 located outside the inversion radius. The reference case with the beam mixing is also given in this figure by dashed curves. In the simulations performed without beam particle mixing the fast rise of the central neutron emission occurs at 22.65s. This rise is caused by the rapid sawtooth-driven influx of tritium which is not compensated by the outward beam flux. The absence of beam outflux leads also to the underestimation of the neutron emission outside the inversion radius after this sawtooth crash (chord n° 7, bottom panel). The subsequent central oscillations of the neutron emission have smaller amplitude and all oscillations observed along the other chords are not reproduced at all without the beam particle mixing.

Another effect tested here is the current profile evolution during the sawtooth crash. This effect is studied by performing the simulations without current mixing and with a partial mixing maintaining $q_0 < 1$ after the crash. The q-profile obtained in simulations with the TRANSP model of partial mixing (Fig.9) displays a region with $q = 1$ after the crash that is close to the profile shape obtained with theoretical incomplete reconnection model [14]. However, two other issues must be taken into account for a proper comparison between the sawtooth model implemented in TRANSP and the model following from the incomplete reconnection [14]. First, the narrow region between the q = 1 surface before reconnection and mixing radius is described differently in TRANSP and in the incomplete reconnection model. In the theoretical model [14] the mixing radius is obtained by extending the region with q = 1 and zero magnetic shear to provide the helical flux conservation while in TRANSP the region with q = 1 (with small, but non-zero shear) is extended in case of partial reconnection. As a result, the mixing radius obtained in TRANSP with the full reconnection model is smaller than the radius obtained with partial reconnection while the opposite effect is expected from the theoretical analysis [14]. The inversion radius is also larger in TRANSP simulations with partial reconnection. The second issue is the transport of energy and particles in the case of incomplete reconnection. On one hand, the rapid return of the hot core region to the centre could reduce the removed energy and particle fraction. But on the other hand, the energy and particle losses can be increased due to the stochastic magnetic field accompanying the incomplete reconnection. In the simulations of the neutron emission presented here the particle losses are assumed to be the same during the full and partial reconnection, i.e. the partial reconnection also produces a strongly off-axis beam particle profile similar to one shown in Fig.5. In such a situation, even a small increase of inversion and mixing radii will produce an important increase of removed beam fraction and therefore, the neutron emission outside the inversion radius. The neutron emission simulated by using the partial mixing and without the current mixing (the q-profile corresponding to this case is shown in Figs. 4 and 9 by dotted curve) is shown in Fig.10 for the central and off-axis chords together with the measurements. The off-axis chord chosen in Fig.10 is located near the mixing radius in the case of full reconnection and the neutron emission along this chord should be sensitive to the slight increase of the mixing radius. Indeed, strong oscillations of the neutron emission are obtained on this chord in the simulations performed without current mixing and with partial mixing. However, the neutron emission measured along the chord n° 8 does not display clear sawtooth oscillations and such oscillations are very weak in the simulations with full mixing (Fig.3 (top)). Thus, the simulations of the neutron emission with the inversion radius and mixed particle fraction estimated with the full reconnection model provide better agreement with the data than the TRANSP model of partial reconnection. The comparison between the full and incomplete reconnection as it is described by theoretical model [14] is still an open issue because the knowledge of particle transport during the incomplete reconnection is needed in addition to the q-profile evolution for proper test of this model.

Another peculiarity of the sawtooth activity is the poloidal asymmetry of the core neutron emission observed after the crash. The Figure 11 shows the neutron emission profiles in the mid-plane as a function of major radius obtained by using the tomographic reconstruction of the neutron measurements performed along the 19 chords. The profiles before the crash are asymmetric and broad at the low field side. The larger neutron emission at the low field side is observed in the region with larger population of trapped deuterium particles and it may be caused by their reaction with tritium. Similar effect – a poloidally asymmetric neutron emission reproducing the banana-like contours in poloidal plane at the beginning of tritium puff has been reported previously [19, 30]. The profile of neutron emission after crash is also broad and asymmetric outside the mid-radius, but in addition, the sawtooth collapse produces the asymmetry in the core region even in the case of initially symmetric core profile (Fig.11, dashed curves). The TRANSP sawtooth model producing a symmetric mixing of particles and energy is not able to reproduce such asymmetry that explains a less accurate prediction of the neutron emission along the in-out core vertical chords. Possible reasons for such an asymmetry (stronger particle losses at the low field side, position of the island, etc.) need further investigation.

4. SAWTOOTH-INDUCED PARTICLE MIXING AT HIGH DENSITY

In contrast to low density plasmas, the oscillations of the neutron emission are not observed at high density even when the ECE oscillations are equally strong (Fig.1(b)). As shown above, the amplitude of the neutron emission oscillations is determined by mixed particle fraction in addition to temperature oscillations, which are fixed by measurements. The mixed trace tritium and deuterium fraction may be different at high and low density depending on the plasma profiles before the crash. The previous analysis of trace tritium transport showed that the transport coefficients exhibit an inverse correlation with plasma density leading to peaked (flat) tritium density profile at low (high) density [19, 29]. In addition, the penetration of neutral beams to the plasma centre is low at high density leading to flat or slightly off-axis beam profile.

The effect of sawtooth crashes in high density plasma is studied in TRANSP simulations with various assumptions on sawtooth mixing similar to the low density case. The simulations of the neutron emission with the full reconnection model have been compared with the simulations performed without the sawtooth mixing, with partial reconnection and with the mixing of main plasma species and trace tritium only. In these simulations the electron temperature measured by the Thomson scattering diagnostics is used because the ECE measurements are available in the narrow core region only (R = 2.5 – 2.95m). The evolution of electron temperature during the sawtooth crash is simulated with the full reconnection model. It should be mentioned also that the electron temperature profile in the core measured with the Thomson scattering diagnostics is in agreement with the ECE measurements.

The simulations of the neutron emission performed with the full reconnection model are compared with the neutron measurements along the 9 horizontal chords in Fig.12. As one can see, both measured and calculated neutron emission does not display the sawtooth oscillations. In this case, the simulations performed under different assumptions on current and particle mixing show a similar evolution of the neutron emission although the q-profiles obtained with and without the current mixing are strongly different. The inversion radius estimated with full reconnection model is smaller at high density, $r_{inv}/a \sim 0.3$, its reduction with density is confirmed also by the ECE and soft X-ray measurements. In contrast to the low density plasma, the neutron emission is insensitive to the beam particle mixing because the beam deuterium profile is flat before the sawtooth crash (Fig.13). The trace tritium penetrates rapidly in the core due to sawtooth crash during the rise phase and its profile changes (Fig.14) similar to the low density case. However, the contribution of the small core region where the tritium density profile is affected by reconnection to the central line integrated neutron emission is not important in a plasma with flat T_i, beam density and neutron emission profiles. Therefore, the oscillations in this region cannot be resolved by using the chord measurements. This also makes difficult to study the sawtooth characteristics at high density.

SUMMARY

The evolution of beam particles and trace tritium during the sawtooth crash in pulses with the NBI heating has been studied numerically using the TRANSP code with the Kadomtsev reconnection model. It was shown that the proper estimation of mixed fraction of these species is important for an accurate prediction of the measured neutron emission oscillations. The fraction of re-distributed species depends on their profiles before the crash. The species with peaked profile are removed from the core due to sawtooth collapse while the species with a hollow profile penetrate towards the core. The amplitude of the oscillations of the neutron emission is determined by the direction and magnitude of the sawtooth-induced beam deuterium and trace tritium fluxes. The removal of both species from the core enhances the neutron emission oscillations while the inward trace tritium flux caused by the sawtooth collapse in combination with the outward deuterium flux is able to cancel these oscillations.

This dynamics of beam and trace particles during the sawtooth crash can explain the peculiarities in the evolution of neutron emission in plasma with different density. In low density plasma the radial profile of the beam deuterium is strongly peaked and a relatively large amount of this species is removed from the core during the crash. The beam particles produce a dominant contribution to the neutron emission oscillations although the trace tritium is able to compensate the outcoming beam particle flux when the tritium profile is hollow. During the decay phase both species are removed from the core amplifying the neutron emission oscillations. In high density plasmas, where the beam density profile is flat, the core neutron emission should be determined mainly by the trace tritium mixing when the tritium profile is hollow. However, the increase of the neutron emission during the sawtooth crash in small core region can not be resolved by the line-integrated measurements in plasma with flat radial profiles. During the decay phase the tritium density profile becomes nearly flat and its modification by the sawtooth collapse is small. That is why the neutron emission oscillations are not observed in high density plasmas during the sawtooth crashes.

The sawtooth oscillations observed at low density can be used for the test of the models describing the magnetic reconnection process (for example full versus incomplete reconnection). The characteristic time of sawtooth collapse indicates that the reconnection occurs in a faster time scale than it is assumed in the full reconnection model [13] that was also observed in other tokamaks. On the other hand, the Kadomtsev model of full reconnection estimates relatively well the fraction of mixed particles matching the neutron emission oscillations. The simulations of the neutron emission are sensitive to this fraction – the small increase of inversion radius (as one obtained with the partial reconnection model in TRANSP) affects strongly the amplitude of the neutron emission oscillations. Since the inversion radius is different with full and incomplete reconnection its lower value in the latter case would lead to under-predicted oscillations of neutron emission unless the particle losses will be artificially enhanced. Thus, it is the energy and particle transport in reconnection region, rather than the q-profile itself is an important parameter for the neutron emission oscillations, and this parameter (if known from the theoretical models) could help to distinguish between the full and incomplete reconnection if the measurements of q-profile with high spatial resolution is not available.

ACKNOWLEDGEMENTS

Dr. V. Yavorskii is warmly acknowledged for useful discussions. This work was performed under the European Fusion Development Agreement, and partly funded by EURATOM and the UK Engineering and Physical Sciences Research Council.

REFERENCES

[1]. S. Von Goeler, *et al*, Phys. Rev. Lett. **33**, 1201 (1974)

[2]. J.A. Wesson, B. Alper, A. W. Edwards, and R. D. Gill, Phys. Rev. Lett., **79**, 5018 (1977)

[3]. A.W. Edwards, et al, Phys. Rev. Lett. **57**, 210 (1986)

[4]. D. Pasini, et al., Nuclear Fusion **30**, 2049 (1999)

[5]. J. O'Rourke, *et al*, Plasma Phys. Contr. Fusion **33**, 289 (1991)

[6]. R.C. Wolf, *et al*, Nuc. Fusion **33**, 663 (1993)

[7]. M.E. Puiatti, *et al*, Plasma Phys. Contr. Fusion **45**, 2011 (2003)

[8]. M.F.F. Nave, *et al*, Nuclear Fusion **43**, 1204 (2003)

[9]. A. Letsch, *et al*, Nucl. Fusion **42**, 1055 (2002)

[10]. F. Bombarda, *et al*, Nucl. Fusion, **38**, 1861 (1998)

[11]. I. Furno, *et al*, Nucl. Fusion **41**, 403 (2001)

[12]. R.F.G. Meulenbroeks, *et al*, Phys. Plasmas **6**, 3898 (1999)

[13]. B.B. Kadomtsev, Sov. Journal Plasma Phys. **1**, 389 (1975)

[14]. F. Porcelli, *et al*, Plasma Phys. Contr. Fusion **38**, 2163 (1996)

[15]. D. Grasso, *et al*, Plasma Phys. Contr. Fusion **41**, 1497 (1999)

[16]. C.G. Gimblett, R. J. Hastie, Plasma Phys. Contr. Fusion **36**, 1439 (1994)

[17]. A.V. Krasilnikov, *et al*, Nuclear Fusion **39**, 1111 (1999)

[18]. M.P. Petrov, *et al*, Phys. Plasmas **6**, 2430 (1999)

[19]. K.-D. Zastrow, *et al*, Plasma Phys. Contr. Fusion **46**, B255 (2004)

[20]. D. Stork, *et al*, *Plasma Physics and Controlled Nuclear Fusion Research*, 2004 (International Atomic Energy Agency, in press), paper OV/4-1

[21]. I. Voitsekhovitch, *et al*, 31st EPS Conference on Plasma Phys., London, 28 June – 2 July 2004 ECA Vol. **28G**, P-1.158 (2004)

[22]. R.J. Goldston, *et al*, J. Comp. Physics **43**, 61 (1981)

[23]. R. Budny, *et al*, Nucl. Fusion **35**, 1497 (1995)

[24]. J.A. Wesson, Nuclear Fusion **30**, 2545 (1990)

[25]. F. Porcelli, Phys. Rev. Lett., **66**, 425 (1991)

[26]. S. Popovichev, *et al*, 31st EPS Conference on Plasma Phys., London, 28 June – 2 July 2004 ECA Vol. **28G**, P-5.173 (2004)

[27]. A. Pankin, *et al*, Comp. Phys. Communications, 2004

[28]. A.A. Korotkov and A.N. Zinov'ev, Sov. Journal Plasma Phys. **15**, 136 (1989)

[29]. I. Voitsekhovitch, X. Garbet, D. C. McDonald, K.-D. Zastrow, *et al*, *Density dependence* of *trace tritium transport in H-mode JET plasma* Physics of Plasmas, 2005, in press

[30]. V. Kiptily, private communication

Table I:
Parameters of NBI heated ELMy H-mode pulses with sawtooth activity.

Pulse No:	B_t, T	I_{pl}, MA	P_{NBI}, MW	Central line density, 10^{19} m^{-3}
61132	1.9	2.35	2.3	2.4
61119	2.25	2.5	14.7	10

Table II:
Characteristic times estimated at the radius with q *= 1 before the sawtooth crash for pulses given in Table I.*

	61132	**61119**
Alfven time, τ_A	0.81μs	1.34μs
Resistive diffusion time, τ_R	10.97s	13.82s
Energy confinement time, τ_E	0.47s	0.45s
Electron collision time, τ_{coll}	0.095μs	0.032μs
Sawtooth reconnection time, τ_{rec}	0.5 - 0.8μs	0.8 - 1.0μs
Sawtooth period, τ_{saw}	0.25 – 0.27s	0.30 – 0.31s

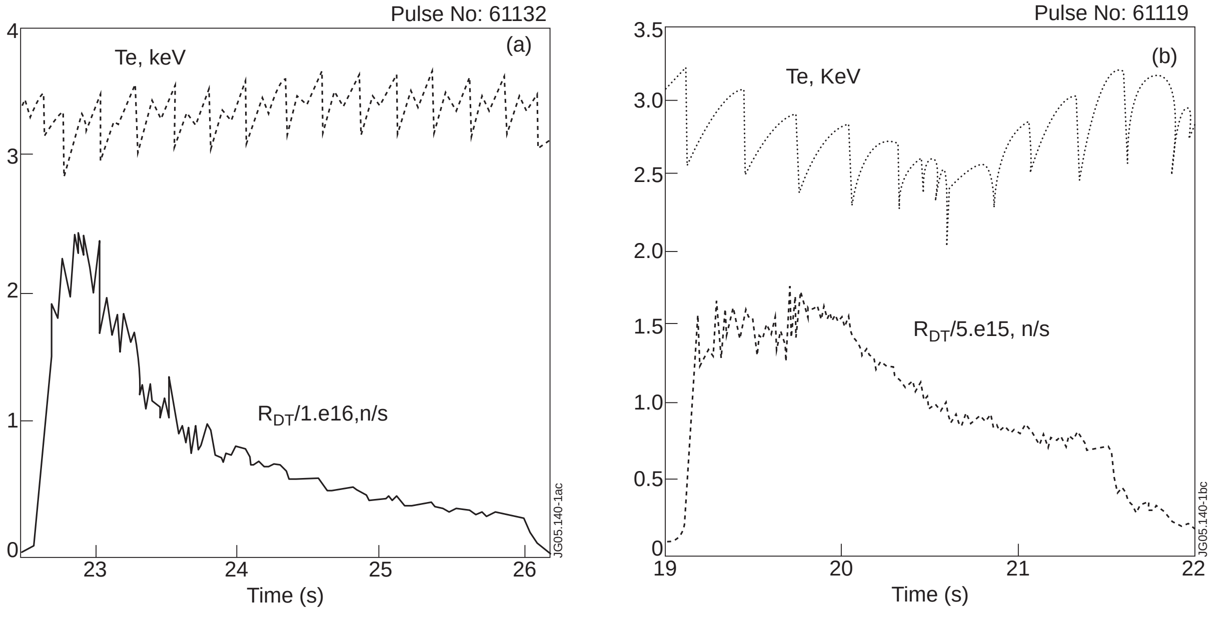

Figure 1: Electron temperature measured by ECE diagnostics in plasma core and DT neutron yield at low (Pulse No: 61132, top) and high (Pulse No: 61119, bottom) density.

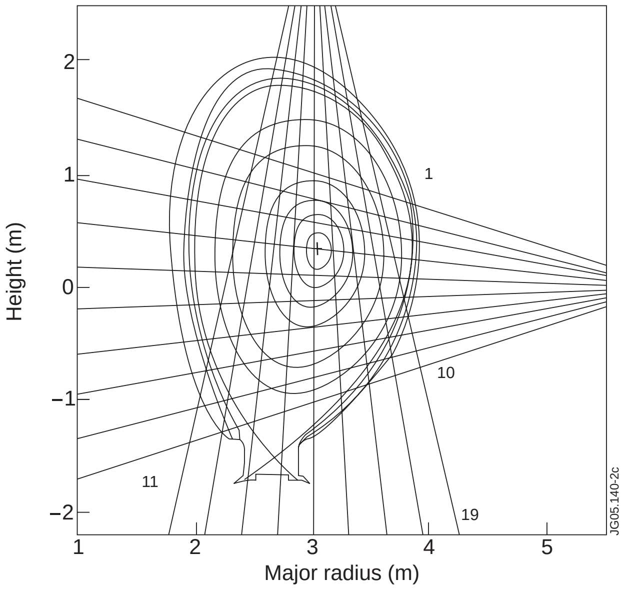

Figure 2: Lines of sight of the neutron profile monitor.

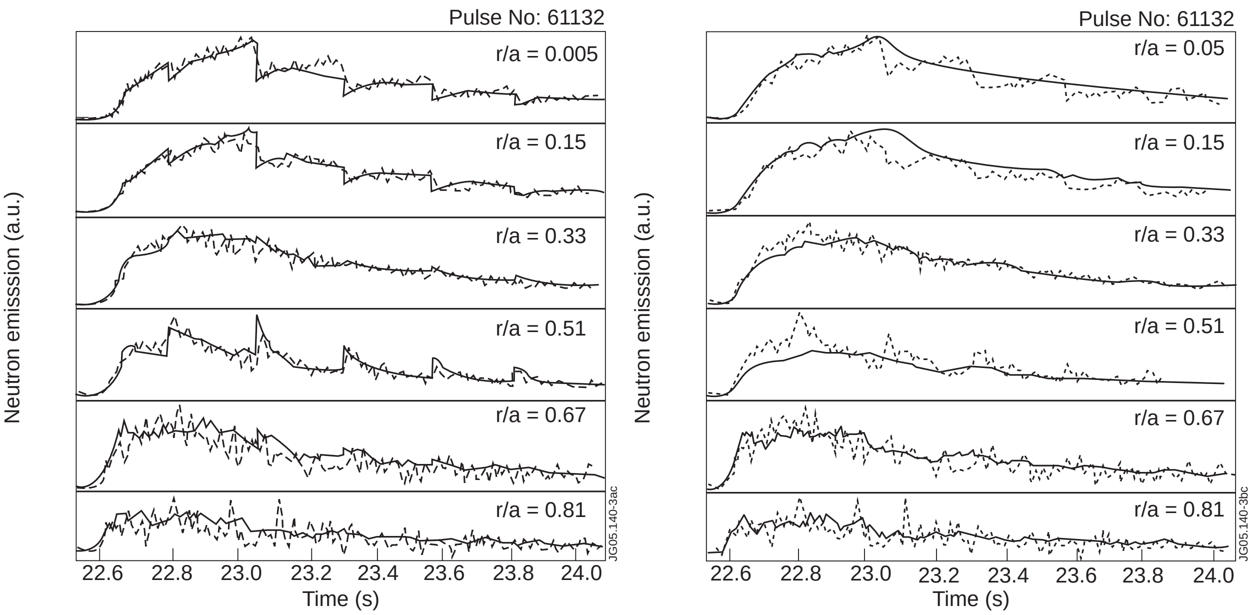

Figure 3: Simulations of the DT neutron emission along the 6 horizontal chords in low density discharge (Pulse No: 61132) obtained with (top) and without (bottom) sawtooth model (bold curves) and comparison with the measurements (dashed curves).

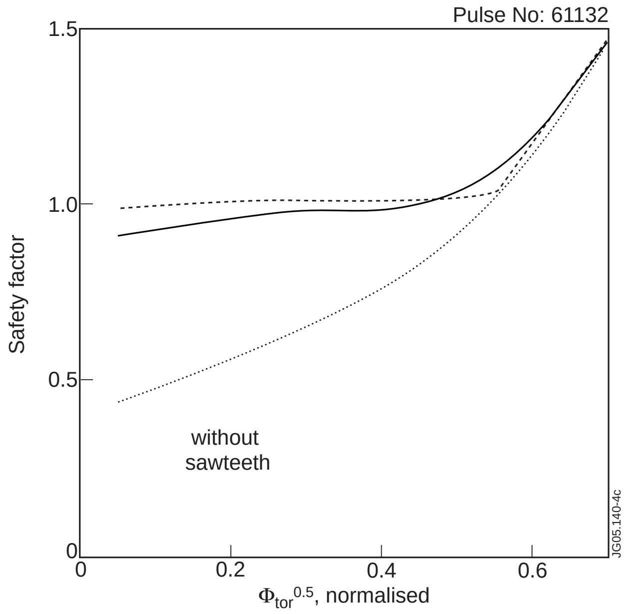

Figure 4: The q*-profile before (solid curve) and after (dashed curve) the sawtooth crash obtained in the simulations shown on the top panel of Fig. 3 (Pulse No: 61132). Dotted curve shows the* q*-profile in the absence of sawtooth mixing.*

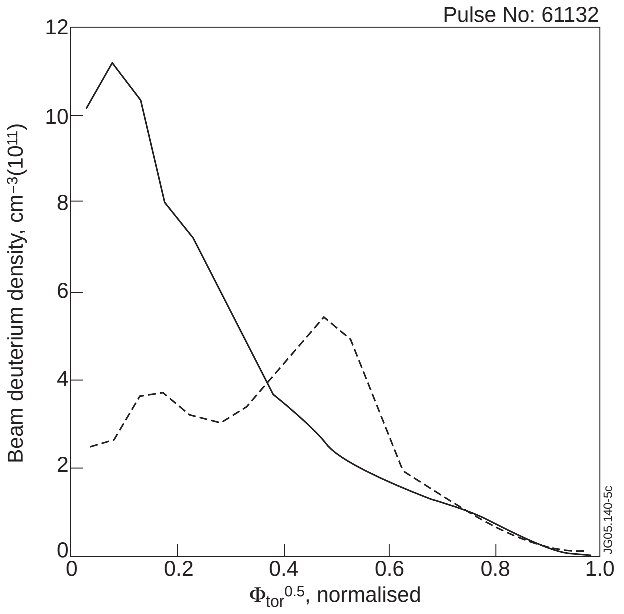

Figure 5: Evolution of beam deuterium profile during the sawtooth crash at 22.65s (Pulse No: 61132). Solid and dashed curves show the profile before and after crash correspondingly.

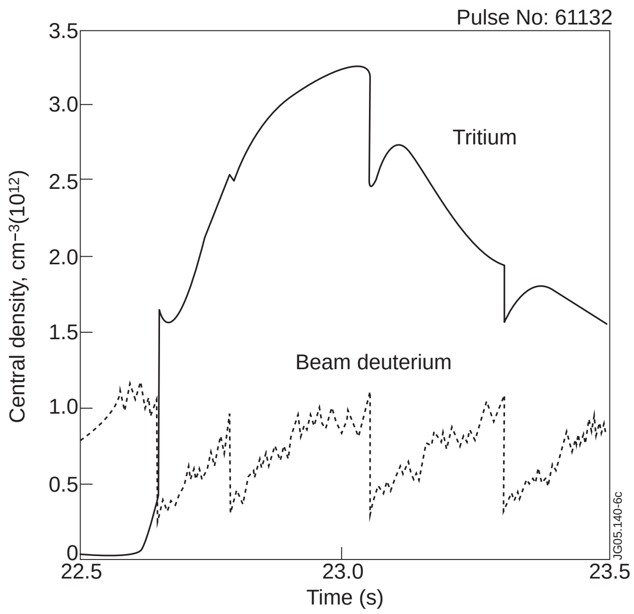

Figure 6: Simulated evolution of central trace tritium density (solid curve) and beam deuterium density (dashed curve) in Pulse No: 61132.

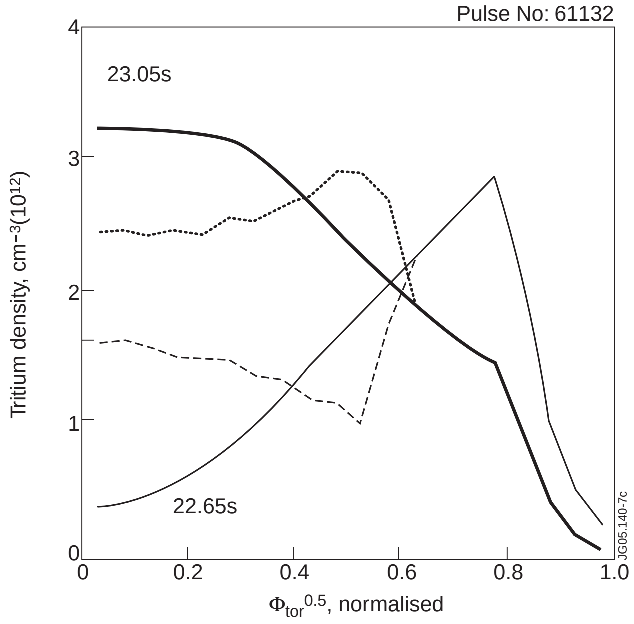

Figure 7: Evolution of tritium density profile during the sawtooth crash occurring during rise (22.65s) and decay (23.05s) phases. Solid and dashed curves show the profiles before and after crash correspondingly.

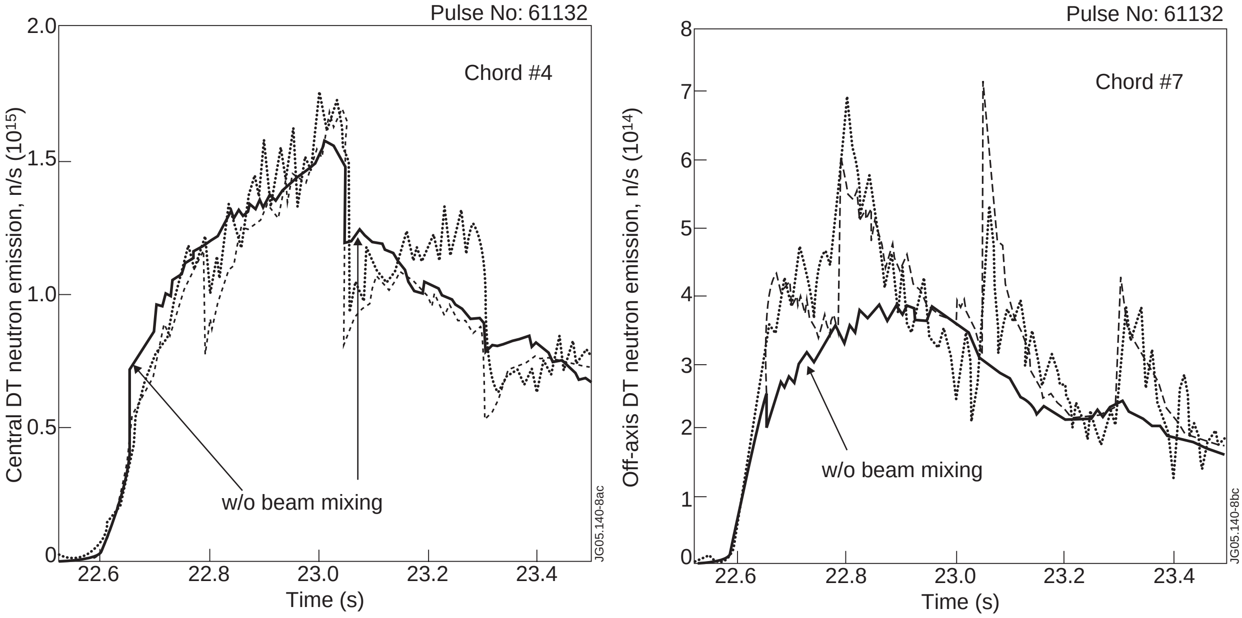

Figure 8: Effect of beam particle mixing in Pulse No: 61132: TRANSP simulations of neutron emission integrated along the central (top) and off-axis chord n°7 (bottom). The simulations performed with the sawtooth mixing of all species are shown by dashed curves, the simulations performed without the beam mixing are shown by bold solid curves. The dotted curves show the measured neutron emission.

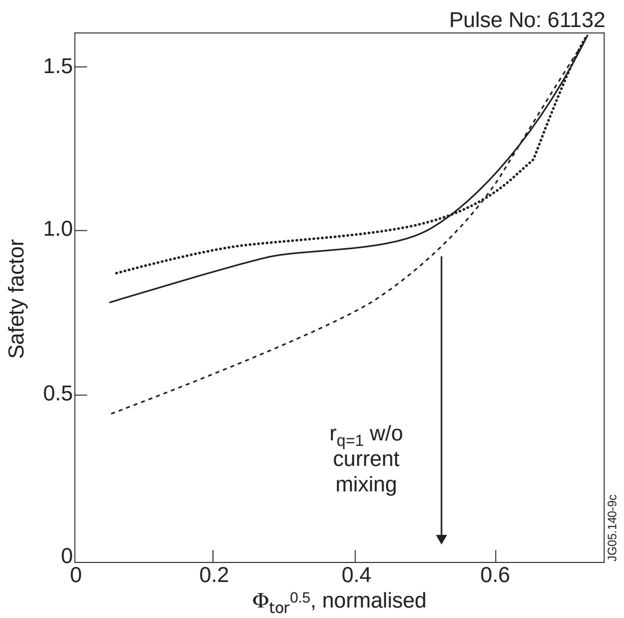

Figure 9: Safety factor profile before (solid curve) and after (dashed curve) the sawtooth crash obtained with partial reconnection (Pulse No: 61132). Dotted curve shows the q profile in the absence of sawtooth mixing (the same as in Fig. 3).

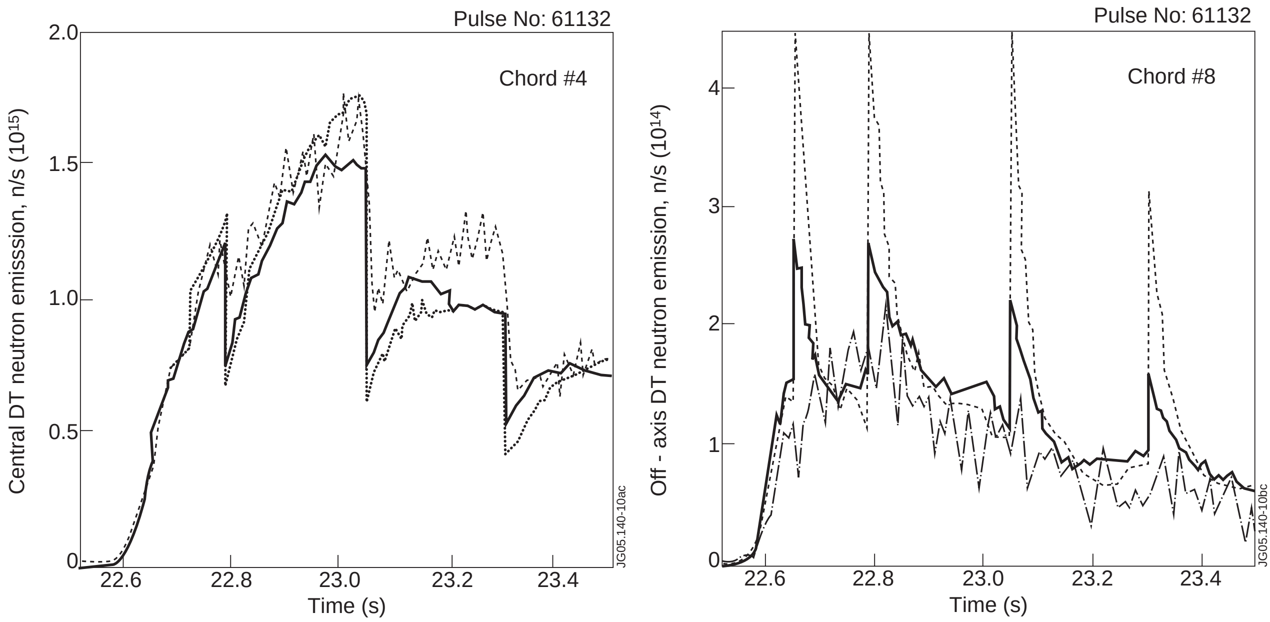

Figure 10: Effect of current mixing in Pulse No: 61132: simulations of neutron emission measured along the central horizontal chord (top) and chord n°8 (bottom). The simulations performed with partial mixing are shown by bold solid curves. The simulations performed without current mixing are shown by dashed curves. The dotted curves show the measured neutron emission.

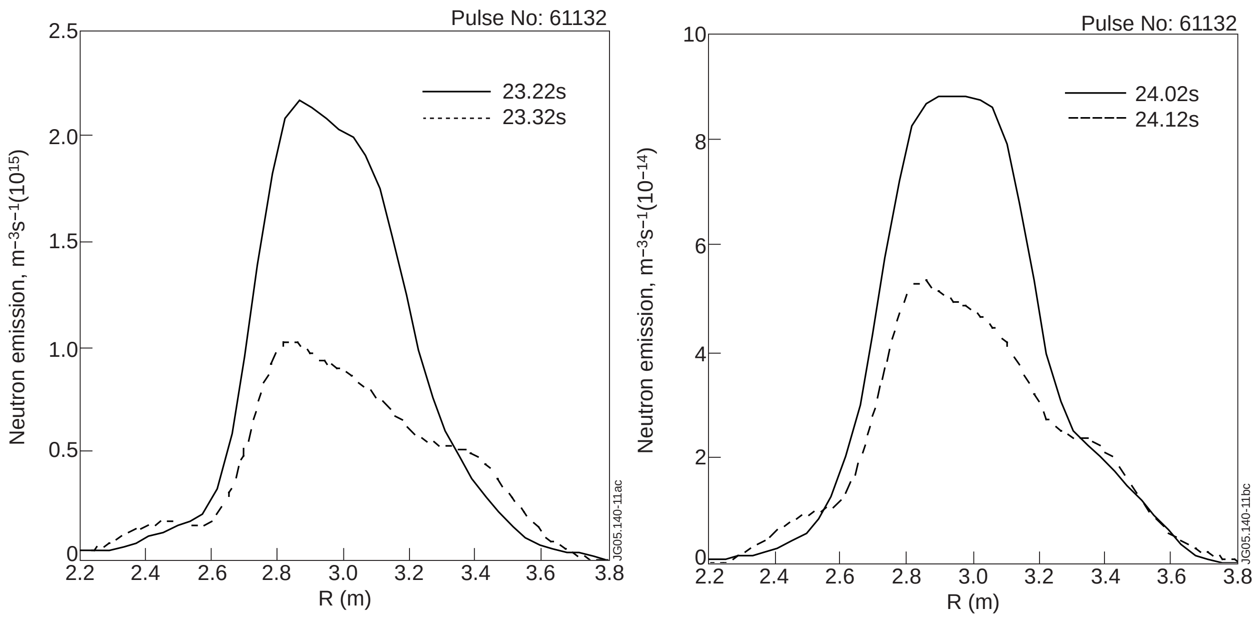

Figure 11: The evolution of the profile of neutron emission along the mid-plane during two sawtooth crashes. These profiles are obtained by using the tomographic reconstruction based on the measurements along the 19 chords. Solid curves show the profiles before the crash, dashed curves show the profiles after the crash. The data are averaged over 50ms around the time indicated on this Figure.

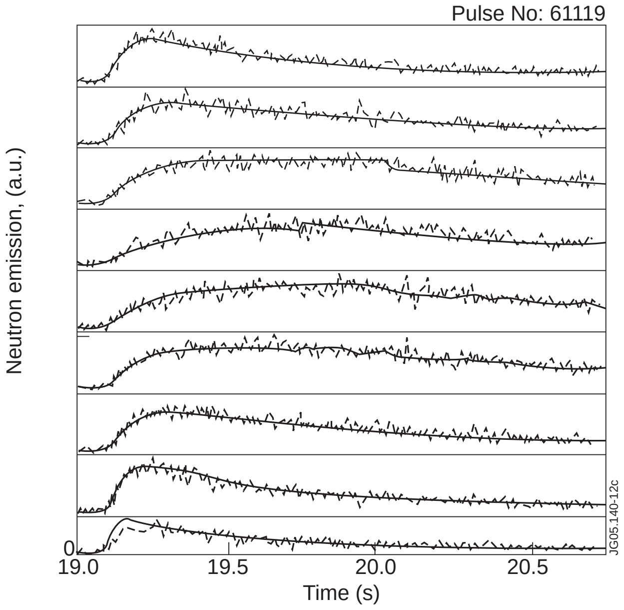

Figure 12: Simulated DT neutron emission along the horizontal chords n° 1 - 9 obtained with full reconnection model (solid curves) and measured neutron emission (dashed curves) for high density Pulse No: 61119.

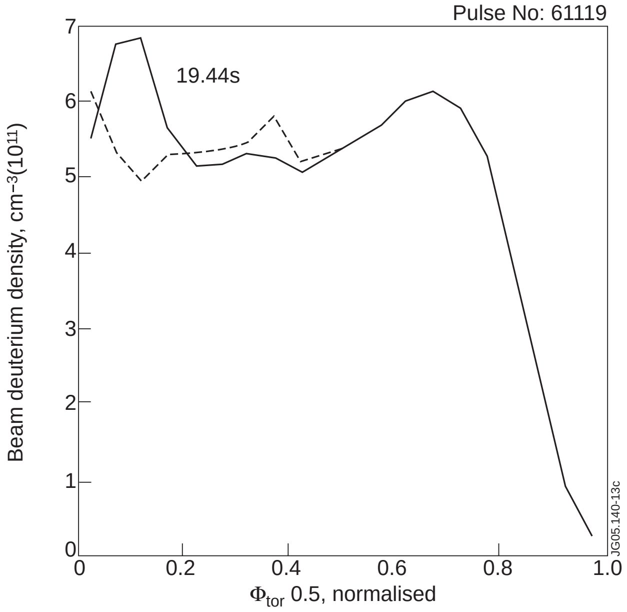

Figure 13: Evolution of beam deuterium during the sawtooth crash occurring at 19.44s (Pulse No: 61119). Solid and dashed curves show the profile before and after crash correspondingly.

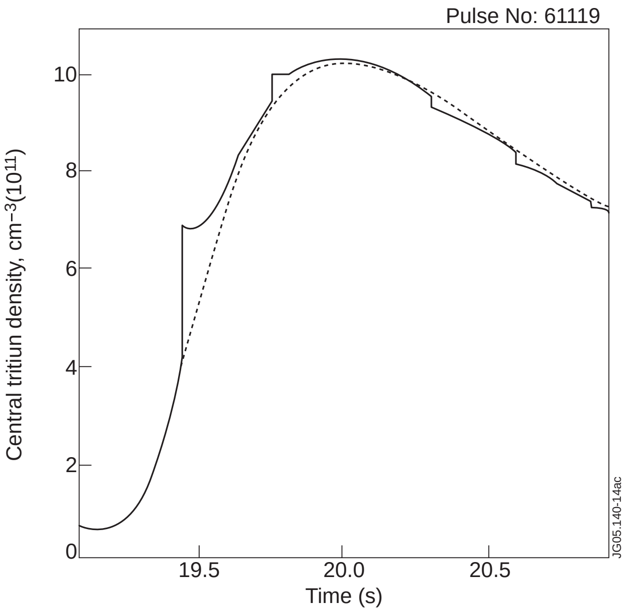

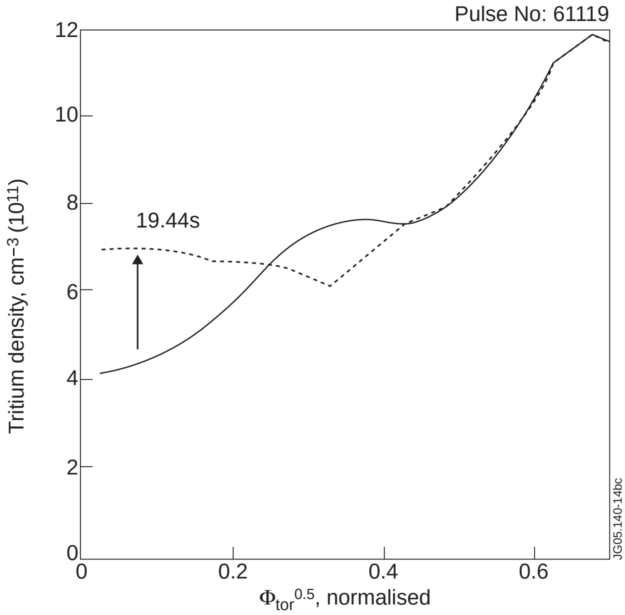

Figure 14: Evolution of central tritium density in simulations with (solid curve) and without (dashed curve) sawteeth (top) and the evolution of tritium density profile during the sawtooth crash occurring during the rise phase (bottom). Solid and dotted curves on bottom panel show the profile before and after the crash correspondingly.